

1 Sample characterizations by topographic imaging

We determined sulfur contents and orthorhombic lattice distortions of $\text{FeSe}_{1-x}\text{S}_x$ single crystals by analyzing the topographic images.

Since sulfur has smaller atomic radius than selenium, sulfur atoms are imaged as depressions in a regular selenium lattice of the STM images (Fig. 1a-e in the main text). Therefore a histogram of the apparent heights at the lattice points may exhibit two peaks; the lower and higher ones correspond to sulfur and selenium, respectively. The sulfur concentration can be calculated from the weights of these two peaks.

For this analysis, we took constant-current STM images over $100\text{ nm}\times 100\text{ nm}$ fields of view with 2048×2048 pixel resolution. Figures 1a-e in the main text are the parts of these images. The precise locations of the lattice points were determined by the Lawler-Fujita algorithm [S1]. The apparent heights at the lattice points were taken from the STM images in which extrinsic long-wave-length height modulations brought by the strains in the crystals etc. were removed by Fourier-filtering out the small \mathbf{q} signals. The obtained histograms shown in Fig. S1a-e exhibit two peaks as expected. We repeated the same analysis for all of the samples we measured and fitted the peaks to obtain the weights. Since the selenium peak consists of a few sub-peaks caused by the randomly-distributed sub-surface sulfur atoms, multiple Gaussian and/or Lorentzian peaks were used for the fitting. The estimated sulfur contents reasonably agree with the results of the energy dispersive X-ray spectroscopy [S2].

Orthorhombic lattice distortions can be estimated from the analyses of the twin boundaries (TB's) [S3]. The model of the crystal structure near the TB is illustrated in Fig. S2a. The orthorhombic lattice distortion $(b_{\text{Fe}} - a_{\text{Fe}})/(b_{\text{Fe}} + a_{\text{Fe}})$ can be calculated from the displacement u associated with the flipping of \mathbf{a}_{Fe} and \mathbf{b}_{Fe} axes across the TB. We found TB's in three samples and evaluated u 's by the Lawler-Fujita algorithm [S1] as described in Ref. [S3] (Fig. S2b). As shown in Fig. S2c, $(b_{\text{Fe}} - a_{\text{Fe}})/(b_{\text{Fe}} + a_{\text{Fe}})$ decreases by a few tens of percent with increasing x , in accord with the decreasing anisotropy in the band structure.

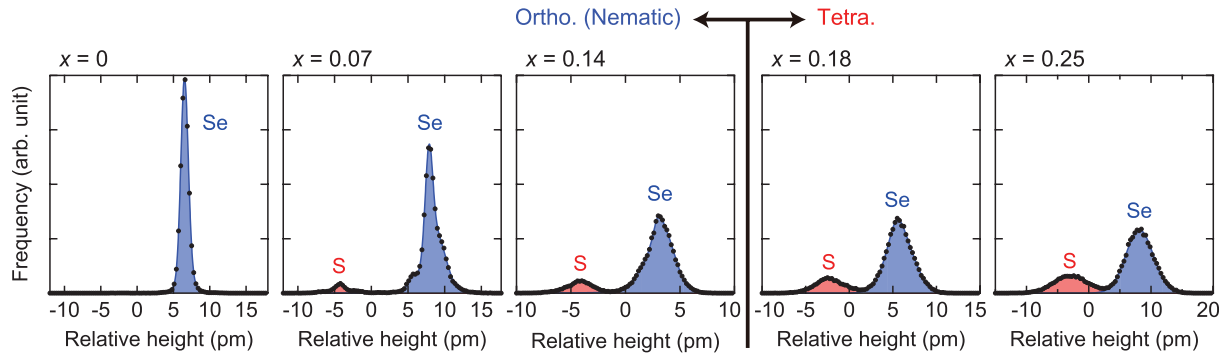


Figure S1: Evolution of the histogram of the apparent heights at the lattice points in $\text{FeSe}_{1-x}\text{S}_x$ single crystals. Black circles represent the experimental data. Filled red and blue curves are the fitted results for the sulfur and selenium peaks, respectively. Because the exact shapes of the tip apex may be different from run to run, ranges of the horizontal axes are not the same.

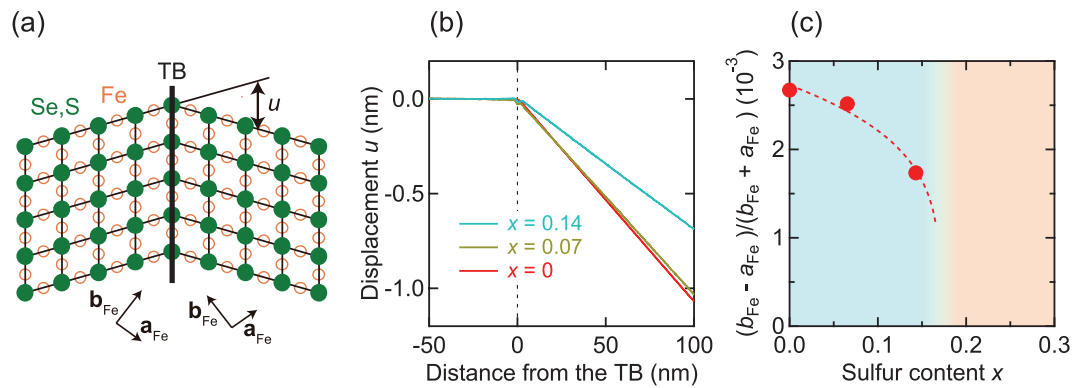


Figure S2: **a**, Model crystal structure near the twin boundary of $\text{FeSe}_{1-x}\text{S}_x$. **b**, Displacement u defined in **a**. **c**, Estimated orthorhombic lattice distortion as a function of x . Dashed line is the guide for the eyes.

2 Energy and sulfur-content evolutions of in-plane QPI patterns

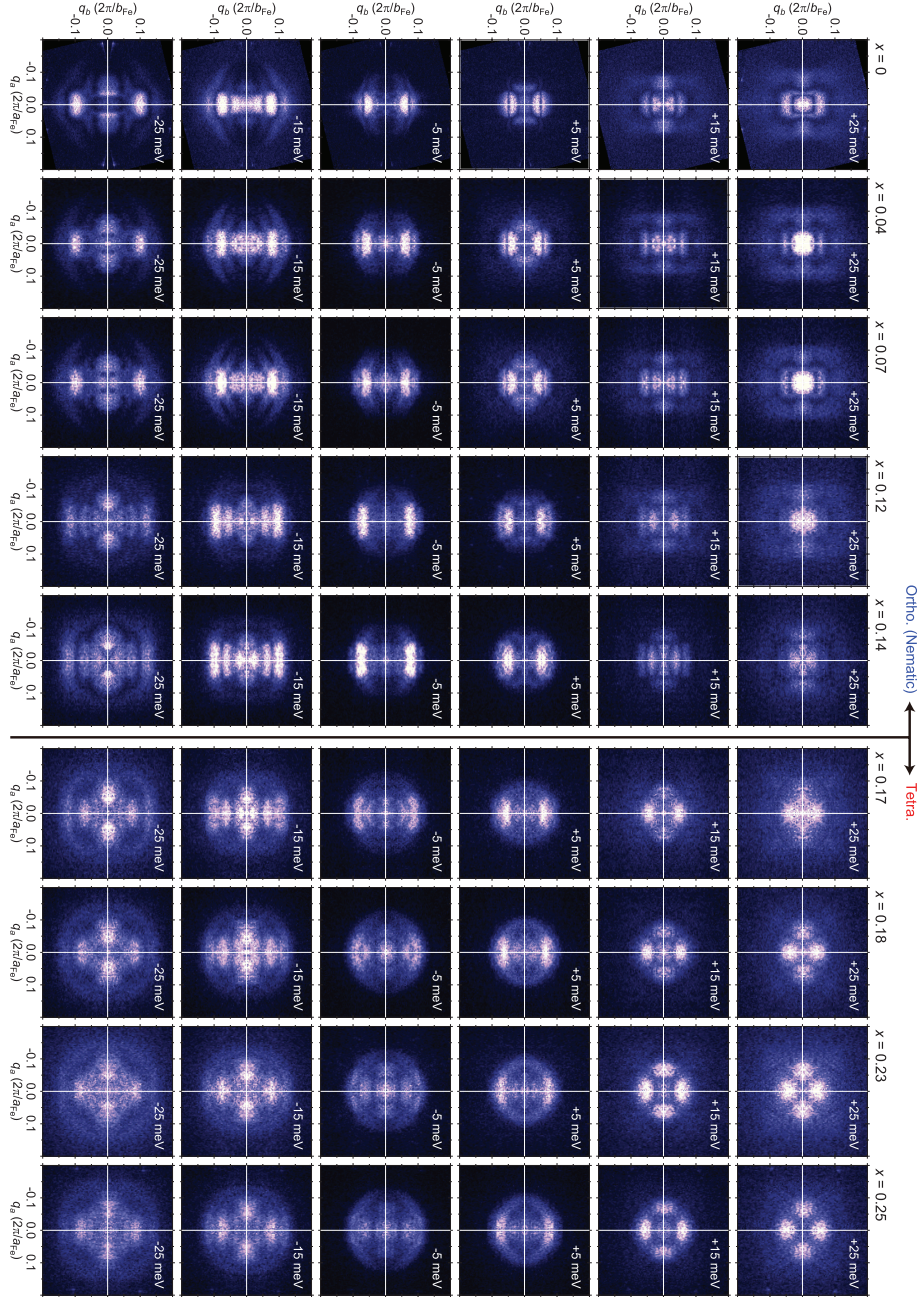


Figure S3: A set of Fourier-transformed images $L_q(\mathbf{q}, E)$ showing the smooth systematic evolutions of the in-plane QPI patterns.

References

- [S1] Lawler, M. J. Fujita, K. Lee, J. Schmidt, A. R. Kohsaka, Y. Kim, C. K. Eisaki, H. Uchida, S. Davis, J. C. Sethna, J. P. & Kim, Eun-Ah *Nature* **466**, 347-351 (2010).
- [S2] Hosoi, S. Matsuura, K. Ishida, K. Wang, H. Mizukami, Y. Watashige, T. Kasahara, S. Matsuda, Y. & Shibauchi, T. Nematic quantum critical point without magnetism in $\text{FeSe}_{1-x}\text{S}_x$ superconductors *Proc. Natl Acad. Sci. USA* **113**, 8139-8143 (2016).
- [S3] Watashige, T. Tsutsumi, Y. Hanaguri, T. Kohsaka, Y. Kasahara, S. Furusaki, A. Sigrist, M. Meingast, C. Wolf, T. Löhneysen, H. v. Shibauchi, & T. Matsuda, Y. *Phys. Rev. X* **5**, 031022 (2016).